Journal of Materials Chemistry C

Accepted Manuscript

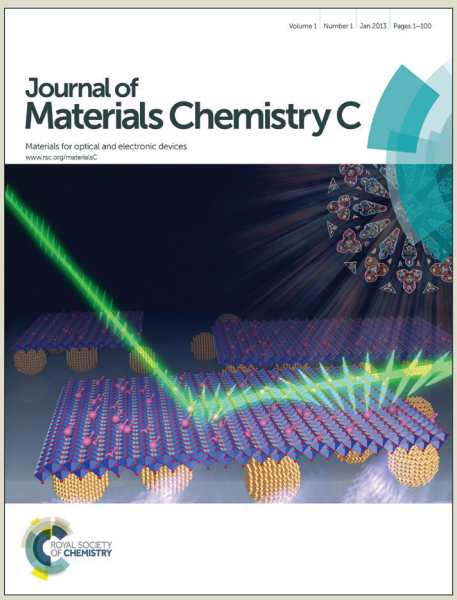

ROYAL SOCIETY OF CHEMISTRY

www.rsc.org/materialsC

Journal Name

COMMUNICATION

Rational Selection of Superparamagnetic Iron Oxide/Silica Nanoparticles to Create Nanocomposite Inductors

Received 00th January 20xx,
Accepted 00th January 20xx

DOI: 10.1039/x0xx00000x

www.rsc.org/

Michael P. Rowe,*[a] Sean Sullivan,[a] Ryan D. Desautels,[b] Elizabeth Skoropata,[b] and Johan van Lierop*[b]

The detailed characterization of core/shell iron-oxide/silica nanoparticles reveals how these superparamagnetic systems are actually composed of a Fe_3O_4 inner core, γ-Fe_2O_3, outer core, iron orthosilicate interphase layer, and exterior silica shell. The performance of a superparamagnetic inductor device is then reported for the nanocomposite formed from the binder-free consolidation of these core/shell nanoparticles.

Introduction

Many of today's modern devices (ranging from cellular phone chargers, to computers, to hybrid automobile powertrain systems) rely on magnetic cores in their power electronic circuitry to control and confine energy in magnetic fields. Due to core losses, a portion of this energy is dissipated and does no work – the principle source of inefficiency in motors, transformers, and inductors.[1] With over 4.5 million hybrid vehicles and an astounding 355 million computers sold just in 2011, even a modest reduction in core loss, summed globally, would represent huge amounts of energy and tremendous savings across society as a whole.

Core losses are due to i) eddy currents that form from the cycling magnetic flux producing its own current (following Faraday's and Lenz's Laws), with the skin effect introducing losses at higher frequencies, combined with ii) magnetic hysteresis from the magnetic material. By hindering the formation of eddy currents and reducing the intrinsic magnetic hysteresis of the core material, core loss can be reduced and efficiency improved. The traditional approach to limiting eddy currents has been to increase the electrical resistivity of the core material.[2,3] Silicon-impregnated steel laminations are the classic magnetic core material that have exemplified this methodology since the early 1900s; an approach that is still used widely.[4]

A more difficult challenge has been reducing magnetic hysteresis losses; state-of-the art techniques established during the heyday of research into the ferrites[3,4] during the 1960s use carefully designed soft magnetic alloys formed into geometries that minimize magnetic flux effects.[5] Nanostructured materials have risen to prominence in the field of magnetism due to the opportunity they offer towards tailoring properties based on constituent component size and shape.[1,6,7] In particular, superparamagnetic nanoparticles with no magnetic hysteresis on the time-scale of the superparamagnetic fluctuations, i.e. no measurable coercivity (H_c), have the potential to outperform conventional soft magnetic materials for particular inductor and transformer applications.[8]

Most applications of superparamagnetic nanoparticles have been biomedical, e.g. developing new drug delivery modalities and contrast enhancement for magnetic resonance imaging.[5-11] However, significantly less work has been done on applications with nanoparticles for electronic and electrical devices.[2,13,14-20] The principal challenge when trying to use nanoparticles for these applications has been maintaining the single-particle superparamagnetic behaviour after the particles have been consolidated into a macroscopic-sized device (so as not to lose the singular magnetic properties of such nanoparticles).

We show here how silica-shell-coated iron-oxide nanoparticles can be consolidated into a nanostructured nanocomposite, by sintering, to form the magnetic core of an inductor, without an additional binder that dilutes the system magnetically. We begin by tuning the thicknesses of silica-shells coating the iron-oxide nanoparticle cores to optimize the magnetism of the final nanocomposite for inductor application. Modification of an iron-orthosilicate interface layer, between the silica shell and iron oxide core, occurs in concert

[a] Toyota Research Institute North America, 1555 Woodridge Ave. Ann Arbor, MI 48105 USA.
[b] Department of Physics & Astronomy, University of Manitoba, Winnipeg, Manitoba, R3T 2N2, (Canada)

* michael.rowe@tema.toyota.com
Electronic Supplementary Information (ESI) available: [details of any supplementary information available should be included here]. See DOI: 10.1039/x0xx00000x

with control of these silica-shell thicknesses. We find that at the device level, upon sintering, the nanoparticle-encapsulating silica matrix constitutes a nanocomposite-structure that provides both increased electrical resistivity and improved thermal stability; both considered advantageous qualities in inductor core design. The inductor fabricated from the superparamagnetic nanocomposite measured for inductance and Q factor exhibited properties consistent with the magnetism of the individual nanoparticles prior to sintering, such that the single-domain character of the nanoparticles has been conserved.

Results and Discussion

The as-prepared core/shell iron-oxide/silica nanoparticles were isolated as loose, free-flowing powders. As detailed below, these nanoparticles were devoid of additional material phases, any sort of extraneous binder, or free silica not associated without an iron-oxide nanoparticle core. Fig. 1a shows typical transmission electron microscopy (TEM) images of the core/shell nanoparticles. Such images identified a log-normal size distribution for the cores, with an average diameter of 4 ± 2 nm, and silica shell thicknesses ranging from 4 to 5 nm, depending on the amount of TEOS used in the synthesis (see Supporting Information Table S1). Rietveld refinements of the nanoparticle systems x-ray diffraction (XRD) patterns established the presence of iron-oxide[20] (see Supporting Information Fig. S1) with a spinel structure (Fd-3m). The lattice constants of 0.837 nm is in keeping with nanoscale Fe_3O_4 or γ-Fe_2O_3, and amorphous silica (SiO_2).[22] Scherrer broadening effects incorporated into the refinements described iron-oxide crystallite sizes in agreement with the TEM results (Fig. 1a). The sintered nanoparticle powders yielded a structurally robust, black nanomaterial. Scanning electron microscopy (SEM) images (Fig. 1b) shows that the process did not alter the nanoparticle structure, with a total nanocomposite core/shell diameter of 10 ± 3 nm particle (in good agreement with the total core/shell sizes of the constituent nanoparticles). The continuous silica matrix formed was, on average, 4.1 ± 1.1 nm thick between iron oxide crystallites. This nanoparticle/silica matrix design effectively controlled the growth of the iron-oxide nanoparticles, as further evidenced by the magnetometry experiments described below. Samples that underwent sintering using overly aggressive hot-press conditions experienced extensive nanoparticle growth, and exhibited unwanted magnetic hysteresis at room temperature.

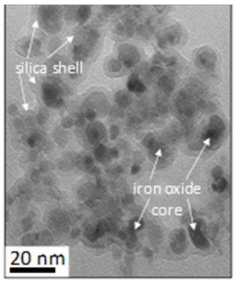

Fig. 1a. Transmission electron microscopy (TEM) image of the iron-oxide nanoparticles encapsulated in silica shells.

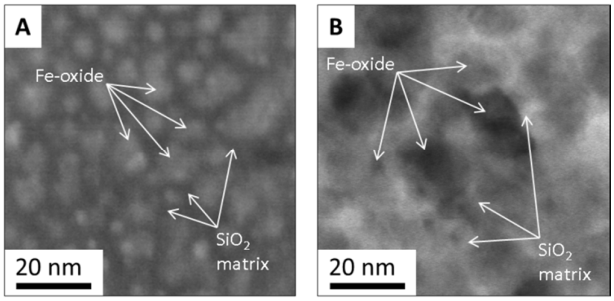

Fig. 1b. A: SEM image of a sintered nanocomposite. Dark areas are the silica matrix and light areas are iron-oxide nanoparticles. B: TEM image of same sample area where the dark areas are now iron-oxide nanoparticles and light areas the silica matrix.

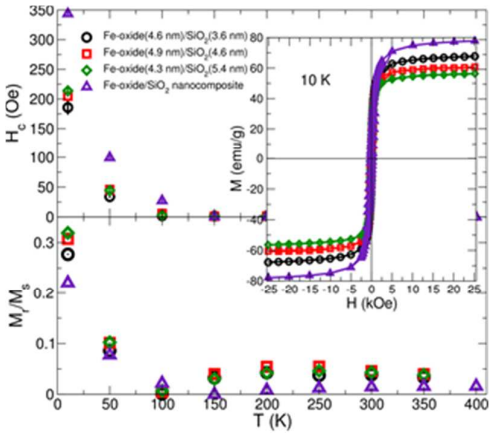

Fig. 2. Coercivity (H_c) as a function of temperature, and the loop squareness factor (M_r/M_s) as a function of temperature for the Fe-oxide/SiO_2 core/shell nanoparticles, and the nanocomposite made from 4.6 nm diameter Fe oxide nanoparticles with 3.6 nm thick silica shells (forming a contiguous silica matrix when sintered). The inset shows the intermediate field-dependence of the 10 K magnetization (M vs H) hysteresis loops from the ± 50 kOe loops that were 50 kOe field-cooled from 400 K. Magnetizations have

been normalized to the total magnetic mass of the samples (see text).

Fig. 2 displays the magnetism of those nanoparticles most relevant for choosing the parent nanoparticles for the device's nanocomposite. The coercivity, H_c, of a system determined from a magnetization-vs-field hysteresis loop must be kept to a minimum (ideally zero). The temperature dependence of H_c (top panel of Fig. 2) from 50 kOe field-cooled hysteresis loops (collected over temperatures from 400 to 10 K) for the as-prepared powders showed an increase in H_c(T) with increasing SiO_2 shell thickness. No measurable field shifts of the hysteresis loops were detected, indicating no significant population of disordered Fe-spins or additional magnetic phases.[23] M_r/M_s(T) (bottom panel of Fig. 2) exhibited an increase with thicker SiO_2 shells. The increase in M_r/M_s(T) with shell thickness could be accounted for by reductions in the magnetic (dipolar) interparticle interactions from increasing core spacing, resulting in single-domain Stoner-Wohlfarth[3] type magnetism with M_r/M_s = 0.5. The overall behaviour of the as-prepared nanoparticles should follow typical thermal fluctuation (i.e. Néel-Brown model) driven magnetism[3], so $H_c = (2K/M_s)(1-(T/T_B)^{1/2})$, where K is the overall magnetic anisotropy, M_s the saturation magnetization of the nanoparticles, and T_B its superparamagnetic blocking temperature. While H_c(T) of the iron-oxide nanoparticles clearly increased with the SiO_2 shell thickness, there was no measurable differences in T_B = 100 ± 5 K between the systems determined from low field DC susceptibility frequency dependent and AC susceptibility measurements (Fig. 3). The intrinsic magnetism of the particle systems, described by M_s and K, must therefore be altered by the SiO_2 shells; an unexpected result. Reducing H_c (and the concomitant magnetic dissipation that can be characterized by the out-of-phase AC frequency response of the magnetization) at all useful frequencies is a prerequisite to a power device application; further insight into M_s and K, and their impact on the magnetization dynamics, is required.

Changes in K values of the different core/shell nanoparticles is provided most simply by analysis of the frequency dependence of the maximum magnetization response (in phase signal of the AC susceptibility, see Fig. 3) that identifies T_B. Interestingly, the typical Néel-Brown prescription could not be used to ascertain physically reasonable K values; the interparticle interactions needed to be accounted for using a Vogel-Fulcher analysis, $v_m/v_0 = \exp[-KV/k_B(T_B - T_0)]$, where v_m and v_0 are the measuring and attempt frequencies of the magnetization reversal, V the nanoparticle's volume, k_B is Boltzmann's constant, and T_0 a 'temperature' that describes the interparticle interaction strength.[25] Fits (see Supporting Information Table S2) showed that the K values track with increasing SiO_2 shell thickness, which correspond to the higher H_c values for the nanoparticle systems. Additionally, increasing SiO_2 shell thickness leads to weaker interparticle interactions. These increasing average core-to-core distances are reflected in decreasing T_o values.

The out-of-phase signal (χ''_{AC}) is a measure of the energy dissipated into the sample during the measurement (see Fig. 3). Note that the nanocomposite presented no clear frequency dependent χ'_{AC}(T) and a factor of 100 decrease in χ''_{AC} (T) compared to the as-prepared powders, signalling that system's superior device properties – hysteretic losses will be reduced significantly. Packing of the nanoparticles into the nanocomposite is substantially increasing the strength of interactions between the nanoparticles, elevating the correlation lengths (and resulting interaction distances) into the strong interaction regime.[24]

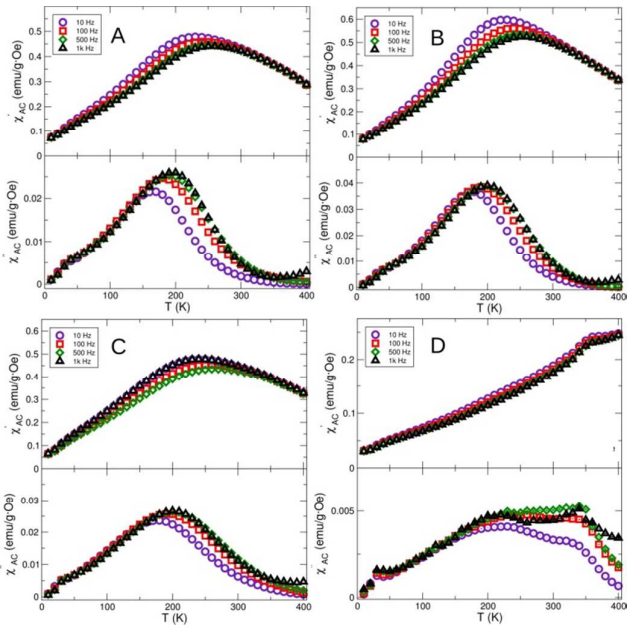

Fig. 3. Temperature dependence of the AC susceptibility collected with a 2.5 Oe drive field at frequencies between 10 and 1000 Hz for nanomaterials of the following dimensions: spectrum A) nanoparticles with 4.6 nm diameter Fe-oxide core and 3.6 nm thick SiO_2 shell; spectrum B) nanoparticles with 4.9 nm diameter Fe-oxide core and 4.6 nm thick SiO_2 shell; spectrum C) nanoparticles with 4.3 nm diameter Fe-oxide core and 5.4 nm thick SiO_2 shell; spectrum D) nanocomposite with 4.6 nm diameter Fe-oxide nanoparticles and 3.6 nm thick SiO_2 matrix. The frequency dependence of the in-phase signal (χ'_{AC}) presents the dynamical freezing effects of the magnetization associated with superparamagnetic blocking, with T_B demarked by the maximum in χ'_{AC}(T).

The question that remains to be addressed to design the optimal nanoparticle for a power device is: Where do the differences in K come from so that H_c and higher frequency hysteretic losses in a nanocomposite can be eliminated? The origin of intrinsic nanoparticle magnetism requires atomic-level information about the magnetism. ^{57}Fe Mössbauer spectroscopy provides the necessary information, and the spectra at 10 K (well below any temperature where spin dynamics of the nanoparticles would alter the spectral line shapes) identify the source of the variations in K between the nanoparticles, shown in Fig. 4. The spectra were fitted initially assuming either stoichiometric Fe_3O_4 or γ-Fe_2O_3 (the only phases consistent with the XRD refinements). Indeed, the only way

to describe consistently the spectra over the range of systems was with a one-to-one mixture of Fe_3O_4 and γ-Fe_2O_3 and a significant fraction of a $Fe^{2.5+}$-based oxide, which could be ascribed to formation of an iron-orthosilicate (e.i. $Si_2Fe_{2.5}O_{12}$).[26-28] The γ-Fe_2O_3 spectral components indicated that the Fe-ions experienced an electric field gradient (e.g. a quadrupole splitting) from broken or distorted coordination, due to surface Fe spins on the nanoparticles (not observed in bulk iron-oxides[29]). Based on these Mössbauer spectra and TEM data, we conjecture that the center of the nanoparticles are made of Fe_3O_4, followed by a layer of γ-Fe_2O_3, with a per-nanoparticle amount of orthosilicate between the iron-oxide strata and silica shell, completed with an outer shell of SiO_2.[27] The hyperfine parameters ascertained from the fits are described in Supporting Information Table S3, with the central finding being ~15%, ~30%, and ~40% of the iron sites were associated with the orthosilicate for nanoparticles with 3.6, 4.9, and 5.4 nm thick silica shells, respectively. The orthosilicate phase provides an overall larger K values for the nanoparticles.

With the compositional information gleaned from the Mössbauer spectra, the iron-bearing phases of the samples can be ascertained, and the magnetometry samples correctly mass normalized. A progressive decrease of the M_s, with increasing SiO_2 shell thickness (Fig. 5), from 70 emu/g to 58 emu/g was measured. Using the Bloch $T^{3/2}$ law[3] to describe $M_s(T)$, the Bloch constant indicated that the Fe-O-Fe superexchange was weakest for the core/shell nanoparticle with the thinnest silica shell (3.5 nm), indicating a decreased magnetic ordering temperature (T_C).

Combining all of the above information, we find that the optimal nanoparticle system is the Fe-oxide nanoparticle with the thinnest silica shell (3.6 nm). It has the most bulk-like M_s, lowest T_C (resulting in lower high frequency hysteresis at higher temperatures), lowest H_c, and lowest K, and the least amount of orthosilicate intermixing. Indeed, hot press sintering this nanoparticle system resulted in the best magnetic response shown by the bulk-equivalent M_s = 81.5 ± 0.2 emu/g, no hysteresis at room temperature, and a minimized M_r/M_s (Fig. 2).

To test the nanocomposite as an inductor, it was machined into a nine millimetre diameter toroid and wrapped with nine windings of enameled copper wire. Four point probe measurement of the electrical resistivity found values on the order of 25 Ωcm; and since a higher electrical resistivity reduces inefficiencies from eddy current formation, this is an approximately 200-times improvement over a typical nanocrystalline, amorphous commercial material.[5] Inductances of 0.670 μH at 1 KHz and 0.454 μH at 5 MHz were measured for the iron oxide/silica nanocomposite device. The Q factor was calculated to be 12 at 1 MHz (Fig. 6). The local increase in Q factor (at 900 and 1000 kHz, see Fig. 6) is a reproducible feature from lower measured resistance, for the inductor device.

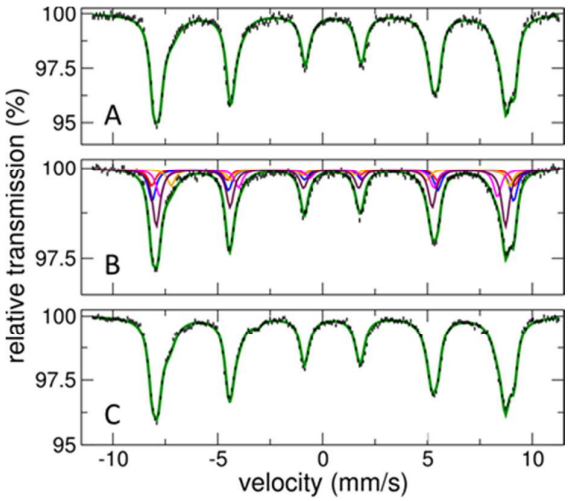

Fig. 4. Transmission Mössbauer spectra collected at 10 K on the Fe-oxide/SiO_2 core/shell nanoparticles with the following dimensions: spectrum A) 4.6 nm diameter Fe-oxide core and 3.6 nm thick SiO_2 shell; spectrum B) 4.9 nm diameter Fe-oxide core and 4.6 nm thick SiO_2 shell; spectrum C) 4.3 nm diameter Fe-oxide core and 5.4 nm thick SiO_2 shell. The solid lines are fits described in the text. An example of the breakdown of spectral components is presented for spectrum B, where red and blue lines are the A- and B-sites of Fe_3O_4, pink and orange lines are the A- and B-sites of γ-Fe_2O_3, and purple is the $Si_2Fe_{2.5}O_{12}$.

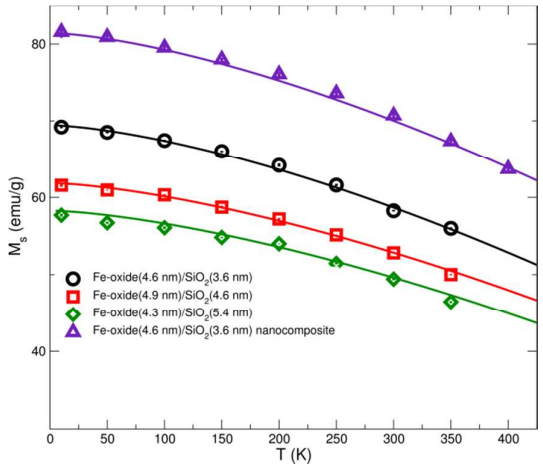

Fig. 5. Iron-oxide mass normalized saturation magnetization as a function of temperature for the as-prepared nanoparticle systems and the nanocomposite. The lines are fits to the $T^{3/2}$ Bloch-law, as described in the text. Bloch constant (that relates the Fe-O-Fe superexchange) dropped from 2.993 ± 0.007 x 10-5 $K^{-3/2}$ for the Fe-oxide (4.6 nm)/SiO_2 (3.6 nm) nanoparticles, to 2.806 ± 0.006 x 10-5 $K^{-3/2}$ for the Fe-oxide (4.6 nm)/SiO_2 (3.6 nm) nanoparticles, to 2.864 ± 0.002 x 10-5 $K^{-3/2}$ for the Fe-oxide (4.3 nm)/SiO_2 (5.4 nm) nanoparticles. The sintered nanocomposite had a Bloch constant of 2.700 ± 0.005 x 10-5 $K^{-3/2}$.

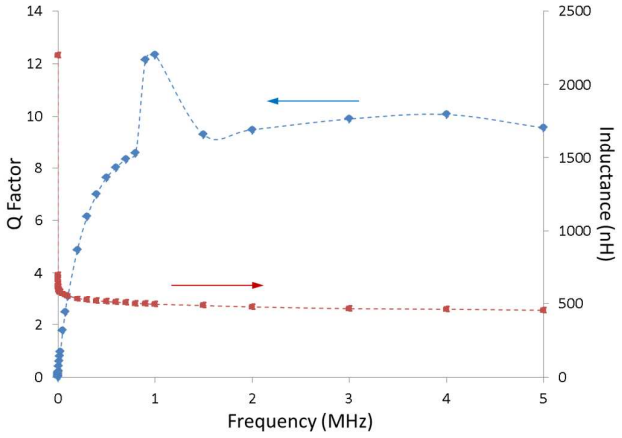

Fig. 6. Plot of Quality factor (Q factor) as it varies with frequency, at room temperature, for the inductor made using a nanocomposite of 4.6 nm diameter Fe-oxide nanoparticles and 3.6 nm thick SiO_2 matrix.

Conclusions

In summary, iron-oxide/silica core/shell nanoparticles were synthesized via a facile wet-process. The influence of a previously unreported interfacial iron orthosilicate layer between the iron-oxide core and silica shell was characterized, giving the first full picture of the system, truly, as a quaternary phase nanoparticle (an Fe_3O_4 inner core, γ-Fe_2O_3 outer core, $Si_2Fe_{2.5}O_{12}$ iron orthosilicate interphase layer, and finally silica outer-shell). While the nanoparticles were all found to exhibit similar blocking temperatures independent of silica-shell thickness, at 10 K their coercivities were increased and magnetic saturations decreased with increasing iron-orthosilicate content. The sintered nanocomposite was shown to be as superparamagnetic as the constituent nanoparticles were prior to consolidation. Testing an inductor fabricated from the nanocomposite determined that its electrical resistivity was quite high in comparison to current widely used commercial ferrite materials, amorphous metals, and nanocrystalline soft magnets. The inductance and Q factors, of the as-fabricated device, were on-par with commercially available inductor cores.

Notes and references

1 A. Makino, T. Kubota, K. Yubuta, *J. Appl. Phys.*, 2011, 109, 07A302.
2 S. Tajima, T. Hattori, M. Kondoh, H. Kishimoto, M. Sugiyama and T. Kikko, *IEEE Trans. Magnets*., 2005, 41, 10.
3 B. D. Cullity and C. D. Graham, Introduction to Magnetic Materials 2nd Edition, John Wiley & Sons Inc., 2009.
4 C. Wm. T. McLyman, Transformer and Inductor Design Handbook 3rd Edition, Marcel Dekker Inc., 2004.
5 T. McLyman, *Transformer and Inductor Design Handbook*, CRC Press, London, 4th edn. 2011.
6 J. Bai and J. Wang, *Appl. Phys. Lett.*, 2005, 87, 152502.
7 K. Zhang, O. Amponsah and M. Arslan, *J. Appl. Phys.*, 2012, 111, 07B525.
8 S. P. Gubin Editor, Magnetic Nanoparticles, Wiley-VCH, 2009.
9 L. Néel, *Ann. Géophys.* 5, 99-136.
10 P. K. Gupta and C. T. Hung, *Life Sci.*, 1989, 44, 175.
11 S. Mornet, O. Lamber, E. Duguet and A. Brisson, *Nano Lett*., 2005, 5, 281.
12 S. Mornet, S. Vasseur, F. Grasset and E. Duguet, *J. Mater. Chem.*, 2004, 14, 2161.
13 J. Lodhia, G. Mandarano, N. J. Ferris, P. Eu and S. F. Cowell, *Biomed. Imaging Interv. J.*, 2012, 6(2):e12.
14 A. S. Teja and P.-Y. Koh, *Prog. Cryst. Growth Ch.*, 2009, 55, 22-45.
15 P. Tartaj, *Eur. J. Inorg. Chem.*, 2009, 333-343.
16 A. S. Eggeman, S. A. Majetich, D. Farrell and Q. A. Pankhurst, *IEEE Trans. Magnets.*, 2007, 43, 6.
17 Z. Zi, Y. Sun, X. Zhu, Z. Yang, J. Dai and W. Song, *J. Magn. Magn. Mater.*, 2009, 321, 1251-1255.
18 S. Ohnuma, H. J. Lee, N. Kobayashi, H. Fujimori and T. Masumoto, *IEEE Trans. Magnets.*, 2001, 37, 4.
19 B. S. Sreeja and S. R. Bonfring *International Journal of Power Systems and Integrated Circuits*, 2011, Vol 1, Special Issue, December.
20 T. Suetsuna, K. Harada, T. Takahashi and S. Suenaga, *J. Appl. Phys.*, 2012, 111, 07A307.
21 Establishing the difference between Fe_3O_4 and γ-Fe_2O_3 in nanoscale iron-oxides is highly problematic as there is essentially only a small difference in tdhe site occupancies of the octahedral and tetrahedral iron sites that identify the differences, and any resultant variations in reflections are smeared out typically due to Scherrer broadening effects.
22 P. Villars and K. Cenzual, *Pearson's Crystal Data: Crystal Structure Database for Inorganic Compounds* (on DVD), Release 2011/12, ASM International®, Materials Park, Ohio, USA.
23 E. Skoropata, R. D. Desautels, C.-C. Chi, H. Ouyang, J. W. Freeland and J. van Lierop, *Phys. Rev. B.*, 2014, 89, 024410.
24 R.D. Desautels, E. Skoropata, M.P. Rowe and J. van Lierop, *J. Appl. Phys.*, 2015, 117, 17C755.
25 S. A. Majetich and M. Sachan, *J. Phys. D: Appl. Phys.*, 2006, 39 R407.
26 C. R.F Lund and J. A. Dumesic, *J. Phys. Chem.*, 1981, 85, 3175.
27 C. R. F. Lund and J. A. Dumesic, *J. Phys. Chem.*, 1982, 86, 130.
28 S. A. Corr, Y. K. Gun'ko, A. P. Douvalis, M. Venkatesan, R. D. Gunning and P. D. Nellist, *J. Phys. Chem.*, 2008, C, 112, 1008.
29 J. Tuček, R. Zobril and D. Petridis, *J. Nanosci. Nanotechnol.*, 2006, 6, 926.

Graphical Abstract: The detailed structure/composition of superparamagnetic Fe_3O_4/γ-Fe_2O_3/iron orthosilicate/silica core/inner-shell/middle-shell/outer-shell nanoparticles and their performance as inductor device is reported.

By Michael P. Rowe*, Sean Sullivan, Ryan D. Desautels, Elizabeth Skoropata and Johan van Lierop*

Title: Rational Selection of Superparamagnetic Iron Oxide/Silica Nanoparticles to Create

Nanocomposite Inductors

Graphical abstract figure: